

Hierarchical Control with Prioritized MPC for Conflict Resolution in Air Traffic Control ^{*}

Georgios Chaloulos, Peter Hokayem, John Lygeros

*Automatic Control Laboratory, Department of Electrical Engineering,
ETH Zürich, Physikstrasse 3, ETL I28, CH-8092, Zürich, Switzerland
(e-mail: {chaloulos, hokayem, lygeros}@control.ee.ethz.ch).*

Abstract: We present a hierarchical solution to the problem of collision avoidance in air traffic control utilizing priority-based Model Predictive Control. First, we abstract the physical aircraft dynamics to simplified ones. Then, we design a centralized model predictive controller that takes into account the physical limitations of the aircraft, such as input constraints and turning rates, as well as the minimum separation safety constraints among the aircraft. We include the effects of bounded winds on the simplified dynamics at the optimization level and show how to exploit the spatial correlation in the wind statistics in order to reduce the conservatism in the separation constraints. This results in a mixed-integer linear program that can be solved online for problems of realistic size. The obtained solution is translated through the flight management system to appropriate inputs to be applied to the physical aircraft dynamics. Monte Carlo simulations are provided to illustrate the effectiveness of the scheme.

1. INTRODUCTION

In futuristic scenarios, it is expected that the air space will be densely populated with various kinds of heterogeneous aircraft. As predicted in Eurocontrol Air Traffic Statistics and Forecast Service [2008], air traffic is expected to double until 2030. This poses serious problems in terms of safety guarantees for the mostly human-operated air traffic control system: the nominal flight plans come closer and closer to each other, while the wind uncertainty affects the actual trajectories. Hence the need for a systematic, scalable, and tractable method of generating collision-free aircraft maneuvers. The problem is further complicated by the additional requirement of respecting pre-assigned priority levels for various aircraft. Following the priority concept proposed in the iFly project (see Cuevas et al. [2008]), higher priority aircraft only maneuver in cases that a maneuver by all lower priority aircraft is not adequate to resolve the conflicting situation.

For commercial flights, safety is translated to all aircraft maintaining at least a minimum prescribed separation while flying; otherwise a conflict occurs. In the literature, several methods for dealing with Conflict Detection and Resolution (CD&R) have been proposed; for a systematic classification and a survey of the research until the 1990s see Kuchar and Yang [2000]. Research on this topic has been focused mainly on simplified mixed integer linear models, in order to allow guarantees on feasibility (see for instance Kuwata et al. [2007], Richards and How [2002]). In Kuwata and How [2010], the authors describe a method to decentralize such problems, while maintaining the feasibility properties of the centralized version of the problem.

Pallottino et al. [2002], divide the problem in two separate ones; one where only speed is regulated and one where only heading angle changes are allowed for the aircraft to maneuver. In Frazzoli et al. [2001] the non-convex quadratically constrained quadratic program, resulting from the separation constraints, is relaxed into an ‘average’ semidefinite program with a randomized solution. More recently, the authors have proposed hierarchical and distributed control to deal with CD&R problems in Chaloulos et al. [2010]. However, the various formulations above either do not incorporate the effect of the wind on the dynamics or have no systematic way of dealing with preassigned priorities or both. Moreover, the actual aircraft dynamics are far from linear. In this paper, we tackle all these issues in a hierarchical framework.

The setup in our paper falls into the general framework of multi-level hierarchical systems (see Mesarović et al. [1970], Findeisen et al. [1980]). We provide a two-level hierarchical collision avoidance algorithm, which takes into account the assigned priorities, the physical limitations of each aircraft, and the minimum allowed separation between any two aircraft. At the highest level, a centralized optimization problem is solved that takes into account all these constraints and generates over a certain prediction horizon N an optimal set of inputs for each aircraft. With the use of linear dynamics, we are able to formulate a mixed-integer linear program (MILP) to be solved periodically. The integer part of the optimization problem arises because of the non-convex nature of the conflict avoidance constraints, the minimum bounds on the aircraft speeds, as well as the priorities assigned to aircraft. Despite the fact that MILP problems can scale very badly, in usual air traffic scenarios most of the integer variables are not adding any active constraints on the problem, thus keeping the computation speed in reasonable levels. Once

^{*} This work is supported by the European Commission under the projects iFly, FP6-TREN-037180 and Feednetback FP7-ICT-223866 (www.feednetback.eu).

the optimal input sequences have been generated for all aircraft, they are pushed down to the lower level in the hierarchy, namely the Flight Management System (FMS). The FMS generates the appropriate inputs and applies them to a simulator of the actual aircraft dynamics. The optimization problem is then resolved periodically and applied in a receding horizon fashion. This hierarchical setup is illustrated in Figure 1.

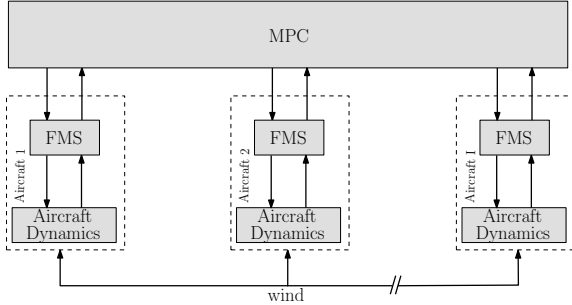


Fig. 1. Hierarchical Multi-Level System

The finite horizon optimization problem solved at each time step falls into the category of Mid-Term Conflict Resolution, with horizons of around 20 minutes. As the actual nonlinear aircraft dynamics are influenced by the wind uncertainty, we need to design a controller that is robust against such uncertainties. Unfortunately, the wind included in the model used for the dynamics is Gaussian with an unbounded support, which renders robust optimization-based control design impossible. As such, we robustify the MILP formulation against most situations, as discussed in the subsequent sections. The use of the correlation structure of the wind is taken into account to reduce conservatism in the problem.

The remainder of this paper is organized as follows. We formulate the problem with all the dynamics and physical constraints in Section 2. We then provide the solution to the priority-based optimization problem to be solved periodically in Section 3. We report our extensive simulation results in Section 4 and include a summary of conclusions of this study in Section 5.

2. PROBLEM FORMULATION

2.1 Dynamics

Consider I aircraft flying within an area of interest, with the following simplified continuous-time dynamics for level flight Lymperopoulos et al. [2007]:

$$\begin{bmatrix} \dot{x}_i \\ \dot{y}_i \\ \dot{v}_i \\ \dot{\psi}_i \\ \dot{m}_i \end{bmatrix} = \begin{bmatrix} v_i \cos(\psi_i) + w_i^x \\ v_i \sin(\psi_i) + w_i^y \\ -\frac{C_{i,D} S_i \rho}{2} \frac{v_i^2}{m_i} + \frac{1}{m_i} T_i \\ \frac{C_{i,L} S_i \rho}{2} \frac{v_i}{m_i} \sin(\phi_i) \\ -\eta_i T_i \end{bmatrix} \quad (1)$$

for $i \in \mathcal{I} \triangleq \{1, \dots, I\}$, where $p_i \triangleq [x_i \ y_i]^\top$ denotes the aircraft position in the horizontal plane, v_i the true aircraft airspeed, ψ_i is the heading angle, m_i the mass, ϕ_i is the bank angle, T_i is the engine thrust, S_i is the surface area of the wings, ρ_i is the air density, η_i is the fuel flow coefficient, and $C_{i,D}$, $C_{i,L}$ are aerodynamic drag and lift coefficients, respectively, whose values depend on aircraft

type and configuration. The system is controlled through ϕ_i and T_i . Noise enters the system via the wind elements w_i^x and w_i^y which are correlated Gaussians, as described in Cole et al. [1998]. As we are concentrating on the level of air traffic controllers, we ignore the effect of wind on the accelerations and turning moments. It can, however, be introduced in the simulation through the so-called wind gradient factors, as shown in Lymperopoulos et al. [2007].

In order to avoid an intractable problem formulation, we abstract the nonlinear dynamics (1) to a linear discrete-time model, based on single integrator dynamics, as follows:

$$p_i(t+1) = p_i(t) + hu_i(t) + hw_i(t), \quad (2)$$

where $p_i(t) = [x_i(t) \ y_i(t)]^\top$, $w_i(t) = [w_i^x(t) \ w_i^y(t)]^\top$, $u_i(t) = [u_i^x(t) \ u_i^y(t)]^\top$ is the velocity input, and h is the sampling period. We denote by

$$\tilde{p}_i(t+1) = \tilde{p}_i(t) + hu_i(t), \quad (3)$$

the dynamics (2) in the absence of wind, and by $\bar{p}_i(t)$ the nominal discrete-time flight plan. The nominal trajectory $\bar{p}_i(t)$ is computed using an ideal straight flight at nominal speed from the current point to the destination p_i^d .

2.2 Velocity Constraints

Corresponding to the simplified dynamics (2), we associate the following two constraints pertaining to the admissible inputs and their rates of change

$$\begin{aligned} \|u_i(t)\|_1 &\geq u_{\min} \\ \|u_i(t)\|_\infty &\leq u_{\max} \\ \|u_i(t+1) - u_i(t)\|_\infty &\leq \delta u \end{aligned} \quad (4)$$

for all $t \in \mathbb{N}$. In general, the input constraints are given in terms of 2-norms and are present to ensure that the aircraft do not stall or fly with extremely high velocities. However, this would lead to an alternative set of constraints in (4), which would be quite inefficient to handle in terms of computation. Thus, we have chosen to approximate the constraints using 1-norm and ∞ -norm constraints. This leads to a more tractable optimization problem, as discussed next, and the relaxations can be further refined using polytopic norms at the expense of more computational effort. The first constraint in (4) is non-convex; however, it can be implemented using the so-called big-M technique and 4 binary variables (similar to Richards and How [2002]), transforming the first input constraint in (4) to

$$\begin{aligned} u_i^x(t) + u_i^y(t) &\geq u_{\min} - M_u c_i^1(t) \\ u_i^x(t) - u_i^y(t) &\geq u_{\min} - M_u c_i^2(t) \\ -u_i^x(t) + u_i^y(t) &\geq u_{\min} - M_u c_i^3(t) \\ -u_i^x(t) - u_i^y(t) &\geq u_{\min} - M_u c_i^4(t) \end{aligned} \quad (5)$$

$$\sum_{\nu=1}^4 c_i^\nu(t) \leq 3, \quad c_i^\nu(t) \in \{0, 1\}$$

where M_u is a sufficiently large number. The last constraint in (5) ensures that at least one of the inequality constraints is active, and consequently that the speed remains above the desired minimum.

2.3 Separation Constraints

With the most critical factor in Air Traffic Control being safety, we need to enforce conflict avoidance constraints. Given a minimum separation among the aircraft Δ (typically 5nm for en-route flights), we pose the following set of constraints at the sampled instants:

$$\|p_i(t) - p_j(t)\|_2 \geq \Delta, \quad (6)$$

for all $t \in \mathbb{N}$ and $i, j \in \mathcal{I}$ with $i \neq j$. However, the constraint (6) does not guarantee that the inter-sample trajectories of (2) do not violate the allowed separation Δ . This is addressed by using a finer time grid: between any two time samples t and $t+1$ we take L subintervals $\left\{t, t + \frac{t}{L}, t + \frac{2t}{L}, \dots, t + \frac{(L-1)t}{L}\right\}$ on which we enforce the constraint (6), i.e., we require the satisfaction of

$$\left\|p_i(t) - p_j(t) + \frac{lh}{L} [u_i(t) + w_i(t) - u_j(t) - w_j(t)]\right\|_2 \geq \Delta, \quad (7)$$

for all $t \in \mathbb{N}$, $l \in \{1, \dots, L\}$, and $i, j \in \mathcal{I}$ with $i \neq j$. Unfortunately, as we have assumed that the noise variables $w_i(t)$ and $w_j(t)$ are normally distributed the constraint (7) is impossible to satisfy for all possible noise realizations. Instead, we enforce the separation constraint with a high level of confidence. Using the triangle inequality, we can conservatively approximate the constraint (7) by

$$\left\|\tilde{p}_i(t) - \tilde{p}_j(t) + \frac{lh}{L} (u_i(t) - u_j(t))\right\|_2 \geq \Delta + \Delta_{i,j}(t, l), \quad (8)$$

where $\tilde{p}_i(t)$ corresponds to the dynamics (3) and

$$\Delta_{i,j}(t, l) = \frac{lh}{L} \|w_i(t) - w_j(t)\|_2. \quad (9)$$

We enforce the constraints (8) for all noise realizations in the 99.7% confidence interval, i.e., for all $w_i^x(t), w_i^y(t), w_j^x(t), w_j^y(t) \in [-3\sigma, 3\sigma]$. With this choice, we obtain the following upper bound

$$\Delta_{i,j}(t, l) \leq 6\sqrt{2}\sigma h \frac{l}{L}. \quad (10)$$

This bound assumes that the noise is uncorrelated in space and may render the constraint (8) conservative.

The spatial correlation of the wind field on the horizontal plane can be described by the following equation (see Cole et al. [1998]):

$$\rho_{xy} (\|\tilde{p}_i(t) - \tilde{p}_j(t)\|_2) = -0.006 + 1.006e^{-\frac{\|\tilde{p}_i(t) - \tilde{p}_j(t)\|_2}{337000}}, \quad (11)$$

where $\|\tilde{p}_i(t) - \tilde{p}_j(t)\|_2$ is the horizontal separation in meters between two aircraft. Since the wind speed enters linearly in our simplified model dynamics, the closer the aircraft are, the smaller the difference in the wind they experience, and, consequently, the smaller the uncertainty on their relative position. Utilizing (11), the difference in the wind speeds experienced by the two aircraft in (9) becomes normally distributed as $(w_{i,x}(t) - w_{j,x}(t)) \sim N(0, \tilde{\sigma}_{i,j}(t))$, where $\tilde{\sigma}_{i,j}(t) = \sigma\sqrt{2 - 2\rho_{xy}(\|\tilde{p}_i(t) - \tilde{p}_j(t)\|_2)}$. Since $\tilde{\sigma}_{i,j}(t)$ depends in a non-convex fashion on the inputs via the dynamics (3), using this exact constraint is not possible. Instead, we use the approximation

$$\bar{\sigma}_{i,j}(t, l) = \sigma\sqrt{2 - 2\rho_{xy}(\|\bar{p}_i(t) - \bar{p}_j(t)\|_2 + h\frac{l}{L}\delta v)}, \quad (12)$$

where $\|\bar{p}_i(t) - \bar{p}_j(t)\|_2$ is the distance that the aircraft would have, if they had followed their nominal flight plans, and δv is a constant related to the maximum allowed change of the airspeed magnitude at each step. Following the same procedure as in equation (10), we obtain the less restrictive

$$\bar{\Delta}_{i,j}(t, l) = 6\sqrt{2}\bar{\sigma}_{i,j}(t, l), \quad (13)$$

with $\Delta_{i,j}(t, l) \geq \bar{\Delta}_{i,j}(t, l)$.

Using this less conservative approximation on the ‘robustifying’ factor $\Delta_{i,j}$, we tighten the non-convex constraint (8), similarly (4), using the norm inequality $\|\cdot\|_2 \geq \|\cdot\|_\infty$, decoupling the noise in the two directions, and the formulation in Richards and How [2002] as:

$$\begin{aligned} \tilde{e}_{i,j}^x(t, l) &= \tilde{x}_i(t) - \tilde{x}_j(t) + \frac{lh}{L} [u_i^x(t) - u_j^x(t)] \\ \tilde{e}_{i,j}^y(t, l) &= \tilde{y}_i(t) - \tilde{y}_j(t) + \frac{lh}{L} [u_i^y(t) - u_j^y(t)] \\ \tilde{e}_{i,j}^x(t, l) &\geq +\Delta + \bar{\Delta}_{i,j}(t, l)/\sqrt{2} - M_{\bar{p}} d_{i,j}^1(t) \\ \tilde{e}_{i,j}^x(t, l) &\leq -\Delta - \bar{\Delta}_{i,j}(t, l)/\sqrt{2} + M_{\bar{p}} d_{i,j}^2(t) \\ \tilde{e}_{i,j}^y(t, l) &\geq +\Delta + \bar{\Delta}_{i,j}(t, l)/\sqrt{2} - M_{\bar{p}} d_{i,j}^3(t) \\ \tilde{e}_{i,j}^y(t, l) &\leq -\Delta - \bar{\Delta}_{i,j}(t, l)/\sqrt{2} + M_{\bar{p}} d_{i,j}^4(t) \\ \sum_{\nu=1}^4 d_{i,j}^\nu(t) &\leq 3, \quad d_{i,j}^\nu(t) \in \{0, 1\} \end{aligned} \quad (14)$$

where $M_{\bar{p}}$ is a sufficiently large number. The last constraint ensures that at least one of the inequality constraints is active, separating the two aircraft by the required distance at least on one of the two axes.

3. PRIORITIZED HIERARCHICAL MPC SOLUTION

3.1 Higher level controller - MPC

In a conflict resolution setting, priorities are often present (see for instance the related work in Hu et al. [2002]), signifying time constraints, fuel constraints, etc. In our setting, inspired by the concept of the iFly project (see Cuevas et al. [2008]), higher priority aircraft only deviate from their flight plan, if the conflict cannot be resolved by all the lower priority ones. We assume that the I aircraft are ordered by increasing priority according to their indices $\{1, \dots, I\}$, i.e., the aircraft with index I has the highest priority. Guided by the setup in Kerrigan et al. [2000], we define I binary variables $\delta_1, \dots, \delta_I$ (one for each aircraft) and given the nominal flight plan sequences $\bar{p}_i(t+k)$ for $k \in \{1, \dots, N\}$, the following set of *deviation* constraints for each aircraft i -th is enforced:

$$\begin{aligned} \|\bar{p}_i(t+k) - \bar{p}_i(t+k)\|_\infty &\leq \epsilon_i(t+k) \\ 0 &\leq \epsilon_i(t+k) \leq M_c \delta_i, \end{aligned} \quad (15)$$

where M_c is a finite constant. The constraint (15) penalizes any deviation of the model (3) from the nominal flight plan due to the designed control action. If a deviation occurs, the binary variable δ_i is set to 1 and results in a higher cost. Given the optimization horizon N we define the cost

$$\mathcal{J}(t) = \underbrace{\sum_{i=1}^I \|\epsilon_i(t+1) \epsilon_i(t+2) \cdots \epsilon_i(t+N)\|_1}_{\text{relaxation of constraints}} + \beta \underbrace{\sum_{i=1}^I 2^{i-1} \delta_i}_{\text{priorities}} \quad (16)$$

where β is a positive scalar given by $\beta = N(I-1)M_\epsilon + 1$. This choice of β ensures that the priorities part of the cost dominates the relaxation of constraints part. Moreover, given the specific structure of weighting, the various binary variables ensure that the satisfaction of higher priority constraints always results in a lower cost than any possible combination of the lower priority constraints, which satisfies our design requirement for priorities.

For the separation constraints, we need to take into consideration the fact that as we advance in the horizon steps, aircraft may have deviated more from their nominal flight plan. Thus, using (13), we get:

$$\bar{\Delta}_{i,j}(t+k|t, l) = 6\bar{\sigma}_{i,j}(t, kL+l), \quad (17)$$

which will be subsequently used in the MPC formulation.

Upon substituting the dynamics (3) into the constraints (14), and by utilizing (17), we obtain the following set of separation constraints along the the optimization horizon N :

$$\begin{aligned} \tilde{e}_{i,j}^x(t+k, l) &= \tilde{x}_i(t) - \tilde{x}_j(t) + \sum_{\tau=t}^{t+k-1} (u_i^x(\tau) - u_j^x(\tau)) \\ &\quad + \frac{lh}{L}(u_i^x(t+k) - u_j^x(t+k)) \\ \tilde{e}_{i,j}^y(t+k, l) &= \tilde{y}_i(t) - \tilde{y}_j(t) + \sum_{\tau=t}^{t+k-1} (u_i^y(\tau) - u_j^y(\tau)) \\ &\quad + \frac{lh}{L}(u_i^y(t+k) - u_j^y(t+k)) \quad (18) \\ \tilde{e}_{i,j}^x(t+k, l) &\geq +\Delta + \bar{\Delta}_{i,j}(t+k|t, l) - M_{\bar{p}}d_{i,j}^1(t) \\ \tilde{e}_{i,j}^x(t+k, l) &\leq -\Delta - \bar{\Delta}_{i,j}(t+k|t, l) + M_{\bar{p}}d_{i,j}^2(t) \\ \tilde{e}_{i,j}^y(t+k, l) &\geq +\Delta + \bar{\Delta}_{i,j}(t+k|t, l) - M_{\bar{p}}d_{i,j}^3(t) \\ \tilde{e}_{i,j}^y(t+k, l) &\leq -\Delta - \bar{\Delta}_{i,j}(t+k|t, l) + M_{\bar{p}}d_{i,j}^4(t) \\ \sum_{\nu=1}^4 d_{i,j}^\nu(t) &\leq 3, \quad d_{i,j}^\nu(t) \in \{0, 1\}, \end{aligned}$$

for all $k \in \{1, \dots, N\}$. Having defined all the required constraints, the main finite-horizon optimization problem to be solved at each time $t \in \{0, 1, 2, \dots\}$ is given by

$$\min_{\substack{u_i(t) \\ i \in \{1, \dots, I\} \\ t \in \{0, \dots, N-1\}}} \left\{ \mathcal{J}(t) \mid (3), (5), (12), (13), (15), (18) \right\}. \quad (19)$$

Problem (19) is an MILP, and hence can be solved effectively for a reasonable traffic scenario.

3.2 Lower level controller - FMS

Once the optimization problem (19) is solved, the resulting control inputs for each aircraft $u_i(t), \dots, u_i(t+N-1)$ are pushed down to the Flight Management System (FMS). Consequently, the FMS generates for the first sampling period h the following thrust and bank angle inputs

$$\begin{aligned} T_i &= \begin{cases} C_T T_{\max} & \text{if } \|u_i(t)\|_2 + \delta_{\text{tol}} > v_i \\ 0.95T_{\max} & \text{if } \|u_i(t)\|_2 - \delta_{\text{tol}} < v_i \\ \frac{C_D S \rho}{2} \|u_i(t)\|_2^2 & \text{else} \end{cases} \\ \Psi_i(t) &= \tan^{-1} \left(\frac{u_i^y(t)}{u_i^x(t)} \right) \\ \phi_i^1 &= k_1 \begin{bmatrix} -\sin \Psi_i(t) \\ \cos \Psi_i(t) \end{bmatrix}^\top \begin{bmatrix} x_i - x_i(t) \\ y_i - y_i(t) \end{bmatrix} + k_2(\Psi_i(t) - \psi_i) \end{aligned} \quad (20)$$

where T_{\max} and C_T are parameters depending on the aircraft type and flight phase of the aircraft (see Eurocontrol Experimental Centre [2004]), δ_{tol} a small tolerance to avoid chattering around the nominal airspeed and k_1, k_2 design parameters of the bank angle controller. As the linear controller ϕ_i^1 may command unrealistically large bank angles, we introduce the following saturation at a given angle $\frac{\pi}{6}$:

$$\phi_i^2 = \min \left\{ \max \left\{ \phi_i^1, -\frac{\pi}{6} \right\}, \frac{\pi}{6} \right\}. \quad (21)$$

Despite the saturation, aircraft may travel in circles in case they deviate too far from their reference path. To prevent this, a further limit, dependent on the heading error is introduced, leading to the final setting for the bank angle:

$$\phi_i = \begin{cases} \min\{\phi_i^2, 0\}, & \pi/2 \geq \psi \geq \frac{\pi}{3} \\ \max\{\phi_i^2, 0\}, & \pi/2 \geq -\psi \geq \frac{\pi}{3} \end{cases} \quad (22)$$

The hybrid controller described in (20) through (22) stabilizes the simplified continuous-time dynamics (1) as shown in Lympelopoulos et al. [2007].

3.3 Overall Hierarchical MPC formulation

The overall proposed scheme is summarized in Algorithm 1.

Algorithm 1 Prioritized Hierarchical MPC Algorithm

Require: $p_i(t), t=0$ and $p_i^d, \forall i \in \{1, \dots, I\}$

- 1: **while** $\exists i$ s.t. $\|p_i(t) - p_i^d\|_2 > \Delta$ **do**
 - 2: Solve the MPC problem (19)
 - 3: Evolve the system according to the FMS and aircraft dynamics (20), (21), and (22) in the interval $[th, (t+1)h[$
 - 4: Set $t = t + 1$
 - 5: Measure new aircraft position $p_i(t)$
 - 6: **end while**
-

4. SIMULATION RESULTS

4.1 Simulation Setup

We constructed a symmetric conflict situation in which six aircraft are initially located on a circle of 300 km radius and are heading to mid-air collision. Without any control action, all aircraft would collide at the center of the circle after approximately 11 minutes. Although rather unrealistic, this scenario allowed us to test the effectiveness of our method as it is quite difficult to tackle due to the very badly initially designed flight plans. The sampling period h is set to 3 minutes and the prediction horizon is set to $N = 6$. The conflict constraints (14) are enforced for $L = 3$ subintervals, i.e. every minute. We used the MILP

solver CPLEX ILOG SA [2008] through the interface package YALMIP (see Löfberg [2005]) for MATLAB on an 8-core cpu for all simulations.

We compared 3 scenarios for 1000 wind realizations:

- (a) Running the proposed algorithm with the aircraft having different priorities and taking into account the correlated nature of the wind.
- (b) Running the algorithm with the aircraft having different priorities as in (a), but ignoring the correlation structure of the wind experienced by aircraft.
- (c) Running the algorithm in the case that all aircraft have the maximum priority level I and taking into account the correlated nature of the wind. Thus, the algorithm will first attempt to minimize the number of aircraft maneuvering and then the magnitude of the maneuver. In this case the cost (16) is modified as:

$$\mathcal{J}^*(t) = \sum_{i=1}^I \|\epsilon_i(t+1) \cdots \epsilon_i(t+N)\|_1 + \beta \sum_{i=1}^I 2^{I-1} \delta_i.$$

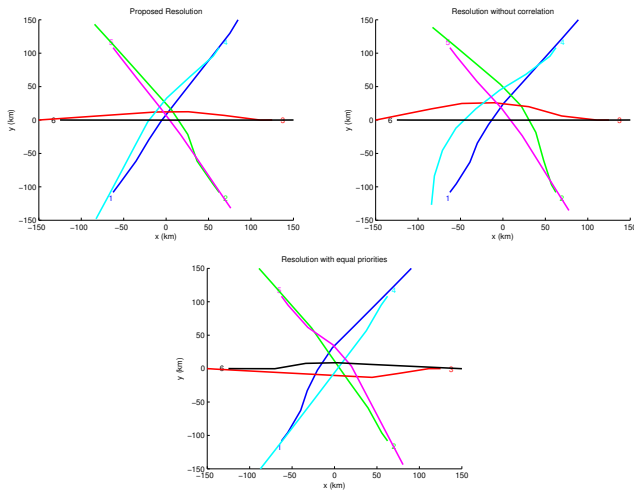


Fig. 2. Resolutions proposed by the three scenarios, (a) (top left), (b) (top right), (c) (bottom).

For visualization purposes, we plot the proposed resolution for the three scenarios (a), (b), and (c) for one wind realization in Figure 2. It can be seen by the plots that taking into account the correlated nature of the wind improves the resolution in terms of reducing the maneuvers needed for each of the aircraft to avoid the conflict. Also, it can be seen that assigning all aircraft the same priority produces trajectories that are fairer to all aircraft in the situation, in the sense that all aircraft contribute similarly to the conflict resolution, through similar extra flying distances.

4.2 Effect of priorities

In order to assess the effect of different priorities, we compared the two scenarios (a) and (c) above in terms of the actual extra distance flown by the aircraft for the cases that the model mismatch and the wind uncertainty did not make the optimization problem infeasible. The results of the Monte Carlo runs are shown as a box-and-whisker diagram in Figure 3.

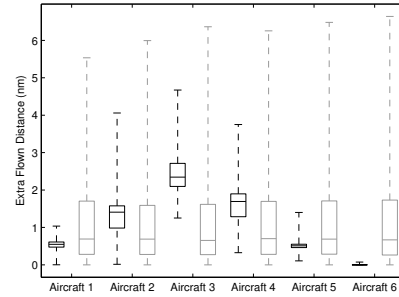


Fig. 3. Extra flown distance per aircraft. For each aircraft, the statistics of the prioritized solution and those of the equal priorities case are depicted on the left (black) and right (grey) boxes and whiskers, respectively.

Case	Mean total extra flown distance (nm)	Actual conflicts	Infeasible cases	Minimum observed separation (nm)	Mean cpu time (mins)	Maximum cpu time (mins)
Scenario (a) (Full model)	6.41	0.21%	0.2%	3.71	1.8	93.3
Scenario (c) (No Priorities)	6.83	0.25%	0.2%	3.32	0.3	12.4

Table 1. Comparison of prioritized and unprioritized resolutions

Even though it may seem that some aircraft perform better on average when all aircraft have the same priority, the standard deviation of the distance among the wind scenarios is bigger than when priorities are used in the formulation. This is explained by the implicit information that priorities carry, making the solution of the optimization problem consistent between the different times that the optimization problem is solved. This is also demonstrated in the first column of Table 1, as the total extra flown distance for each scenario is better on average when priorities are introduced. Furthermore, Table 1 suggests that despite the model mismatch and enforcing the constraints every minute (instead of continuously), very few conflicts were not detected and promptly resolved by the algorithm, while in the few cases that this happened, separation was violated less when priorities were used. However, a clear disadvantage when introducing priorities is that the computational times are higher.

4.3 Effect of wind correlation

We then compared the scenarios (a) and (b) above, in order to assess how much ignoring the correlation structure described in this study can affect the performance of the resolution algorithm. As Figure 4 suggests, the aircraft may have to deviate more than twice as much as they would have to in the case that the correlation structure is implemented in the optimization. Table 2, summarizes the results for various wind realizations. This highlights the advantage of implementing the wind correlation structure in the optimization, since otherwise the aircraft are forced to perform much more conservative maneuvers. The only advantage of the uncorrelated wind case is the better behavior against infeasibility; in no case did the aircraft violate the required separation, but resulting more cases

Case	Mean total extra flown distance (nm)	Actual conflicts	Infeasible cases	Minimum observed separation (nm)	Mean cpu time (sec)	Maximum cpu time (sec)
Scenario (a) (Full model)	6.41	0.21%	0.2%	3.71	1.8	93.3
Scenario (b) (Uncorrelated)	17.9	0%	0.7%	6.69	9	541.1

Table 2. Comparison of using and ignoring the correlation structure of the wind

that the algorithm could not resolve. On the other hand, the computation times needed are much higher.

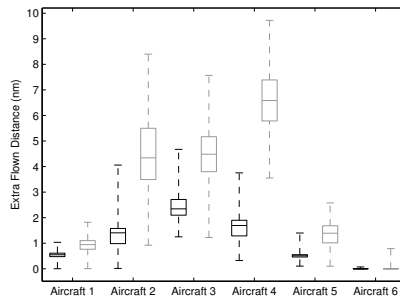


Fig. 4. Extra flown distance per aircraft. For each aircraft, the statistics of the correlated model and those of the uncorrelated model are depicted on the left (black) and right (grey) boxes and whiskers, respectively.

5. CONCLUSIONS

We presented a hierarchical MPC scheme to deal with conflict detection and resolution. We utilized a simplified version of the aircraft dynamics that allows an MILP formulation for the problem. We also introduced priorities in a systematic way into the optimization problem and took into account the wind correlation in order to reduce the conservatism of the proposed resolution. We provided comparative studies that illustrate the effectiveness of our approach.

Ongoing research focuses on addressing constraints relaxation on the event when a robust solution for the algorithm cannot be found. Furthermore, possible decentralization schemes are being explored. It is also interesting to investigate the behavior of our method on more realistic large-scale air traffic scenarios.

REFERENCES

- G. Chaloulos, P. Hokayem, and J. Lygeros. Distributed hierarchical MPC for conflict resolution in air traffic control. In *American Control Conference (ACC), 2010*, pages 3945–3950. IEEE, 2010.
- R.E. Cole, C. Richard, S. Kim, and D. Bailey. An assessment of the 60 km rapid update cycle (RUC) with near real-time aircraft reports. Technical Report NASA/A-1, MIT Lincoln Laboratory, July 1998.
- G. Cuevas, I. Echegoyen, J. García, P. Cásek, C. Keirath, F. Bussink, and A. Luuk. Autonomous Aircraft Advanced (A³) ConOps. Technical Report Deliverable D1.3, iFly Project, 2008.
- Eurocontrol Air Traffic Statistics and Forecast Service. *Long-Term Forecast: IFR Flight Movements 2008-2030*. December 2008. URL <http://www.eurocontrol.int/statfor/gallery/content/public/forecasts/Doc302 LTF08 Report Vol1 v1.0.pdf>. [Online].
- Eurocontrol Experimental Centre. *User Manual for the Base of Aircraft Data (BADA)*. 2004. URL <http://www.eurocontrol.fr/projects/bada/>.
- W. Findeisen, F. N. Bailey, M. Brdyś, K. Malinowski, P. Tatjewski, and A. Woźniak. *Control and Coordination in Hierarchical Systems*. John Wiley & Sons, 1980.
- E. Frazzoli, Z. H. Mao, J. H. Oh, and E. Feron. Aircraft conflict resolution via semi-definite programming. *AIAA J. of Guidance, Control, and Dynamics*, 24(1):79–86, 2001.
- J. Hu, M. Prandini, and S. Sastry. Optimal Coordinated Maneuvers for Three-Dimensional Aircraft Conflict Resolution. *AIAA Journal of Guidance, Control and Dynamics*, 25(5), 2002.
- ILOG SA. CPLEX 11.0 Users Manual. Technical report, Gentilly, France, 2008.
- E.C. Kerrigan, A. Bemporad, D. Mignone, M. Morari, and J.M. Maciejowski. Multi-objective prioritisation and reconfiguration for the control of constrained hybrid systems. volume 3, pages 1694–1698, Chicago, IL, USA, June 2000.
- J.K. Kuchar and L.C. Yang. A review of conflict detection and resolution methods. *IEEE Transactions on Intelligent Transportation Systems*, 1(4):179–189, 2000.
- Y. Kuwata and J. P. How. Cooperative distributed robust trajectory optimization using receding horizon milp. *IEEE Transactions on Control Systems Technology*, 2010. to appear.
- Y. Kuwata, A. Richards, T. Schouwenaars, and J.P. How. Distributed robust receding horizon control for multi-vehicle guidance. *IEEE Transactions on Control Systems Technology*, 15(4):627–641, 2007.
- J. Löfberg. YALMIP: A toolbox for modeling and optimization in MATLAB. In *2004 IEEE International Symposium on Computer Aided Control Systems Design*, pages 284–289. IEEE, 2005.
- Ioannis Lympelopoulos, Andrea Lecchini, William Glover, Jan Maciejowski, and John Lygeros. A stochastic hybrid model for air traffic management processes. Technical Report CUED/F-INFENG/TR.572, Department of Engineering, Cambridge University, February 2007.
- M. D. Mesarović, D. Macko, and Y. Takahara. *Theory of Hierarchical, Multilevel, Systems*, volume 68 of *Mathematics in Science and Engineering*. Academic Press, New York, NY, 1970.
- L. Pallottino, E. M. Feron, and A. Bicchi. Conflict resolution problems for air traffic management systems solved with mixed integer programming. *IEEE Transactions on Intelligent Transportation Systems*, 3(1):3–11, mar. 2002.
- A. Richards and J.P. How. Aircraft trajectory planning with collision avoidance using mixed integer linear programming. In *American Control Conference*, volume 3, pages 1936–1941, Anchorage, Alaska, USA, May 2002. IEEE.